Acta Astronautica 192 (2022) 30–46

Contents lists available at ScienceDirect

Acta Astronautica

journal homepage: www.elsevier.com/locate/actaastro

Research paper

RoboCrane: A system for providing a power and a communication link between lunar surface and lunar caves for exploring robots

Pablo F. Miaja [a], Fermin Navarro-Medina [b], Daniel G. Aller [a], Germán León [a], Alejandro Camanzo [c], Carlos Manuel Suarez [d], Francisco G. Alonso [d], Diego Nodar [e], Francesco Sauro [f], Massimo Bandecchi [g], Loredana Bessone [h], Fernando Aguado-Agelet [c], Manuel Arias [a,*]

[a] Electrical Engineering Department, University of Oviedo, 33204, Spain
[b] Aerospace Engineering Area, School of Aeronautic and Space Engineering, Universidade de Vigo. As Lagoas s/n, Ourense, 32004, Spain
[c] Escola de Enxeñaría de Telecomunicación, Universidade de Vigo, 36310, Spain
[d] Mechanical engineering Department, University of Oviedo, 33204, Spain
[e] Alén Space, Edificio Tecnológico Aeroespacial, Rúa das Pontes 6, Oficina 2.03, 36350, Spain
[f] Department BIGEA, University of Bologna, Italy
[g] European Space Agency (ESA), TEC-S, Directorate of Technology, Engineering & Quality, ESTEC, Keplerlaan 1, 2200 AG Noordwijk, Netherlands
[h] European Space Agency (ESA), HRE-OT, Linder Höhe, D-51147 Cologne, Germany

ARTICLE INFO

Keywords:
Lunar lava tubes
Skylight
Lunar caves
Crane
RoboCrane
Exploration
Robot swarm
Wireless charger

ABSTRACT

Lava caves are the result of a geological process related to the cooling of basaltic lava flows. On the Moon, this process may lead to caves several kilometers long and diameters of hundreds of meters. Access to lava tubes can be granted through skylights, a vertical pit between the lava tube and the lunar surface. This represents an outstanding opportunity for long-term missions, for future permanent human settlements, and for accessing pristine samples of lava, secondary minerals and volatiles. Given this, the ESA launched a campaign through the Open Space Innovation Platform calling for ideas that would tackle the many challenges of exploring lava pits. Five projects, including Robocrane, were selected.

Solar light and direct line of sight (for communications) with the lunar surface are not available inside lava tubes. This is a problem for any robot (or swarm of robots) exploring the lava tubes. Robocrane tackles both problems by deploying an element (called the Charging head, or CH) at the bottom of the skylight by means of a crane. This CH behaves as a battery charger and a communication relay for the exploring robots. The required energy is extracted from the crane's solar panel (on the surface) and driven to the bottom of the skylight through an electrical wire running in parallel to the crane hoisting wire. Using a crane allows the system to deal with unstable terrain around the skylight rim and protect the wires from abrasion from the rocky surface and the pit rim. The charger in the CH is wireless so that the charging process can begin as soon as any of the robots get close enough to the CH. This avoids complex and time-consuming docking operations, aggravated by the skylight floor orography. The crane infrastructure can also be used to deploy the exploring robots inside the pit, reducing their design constraints and mass budget, as the robots do not need to implement their own self-deployment system. Finally, RoboCrane includes all the sensors and actuators for remote operation from a ground station.

RoboCrane has been designed in a parametric tool so it can be dynamically and rapidly adjusted to input-variable changes, such as the number of exploring robots, their electrical characteristics, and crane reach, etc.

* Corresponding author.
E-mail addresses: fernandezmiapablo@uniovi.es (P.F. Miaja), fermin.navarro.medina@uvigo.gal (F. Navarro-Medina), garciaadaniel@uniovi.es (D.G. Aller), gleon@uniovi.es (G. León), camanzo.marino.alejandro@uvigo.es (A. Camanzo), csuarez@uniovi.es (C.M. Suarez), diego.nodar@alen.space (D. Nodar), francesco.sauro2@unibo.it (F. Sauro), Massimo.Bandecchi@esa.int (M. Bandecchi), Loredana.Bessone@esa.int (L. Bessone), faguado@tsc.uvigo.es (F. Aguado-Agelet), ariasmanuel@uniovi.es (M. Arias).

https://doi.org/10.1016/j.actaastro.2021.11.023
Received 6 August 2021; Received in revised form 1 October 2021; Accepted 17 November 2021
Available online 2 December 2021

1. Introduction

In the last two decades, various satellite missions have confirmed the presence on the Moon of peculiar pits that could allow access to subsurface voids [1,2]. This discovery has led notable scientific debate on the geological nature of these cavities and on what may be found in their interior [3]. Since the early seventies several authors [4–6] have argued that lunar rilles in the Maria could be associated with collapsed lava tubes. Therefore, lunar pits may represent potential entrances to volcanogenic underground channels. Lava tubes or pyroducts on Earth are the result of a geological process in which the surface of a basaltic lava flow hardens as a consequence of rapid cooling, forming a superficial crust [7]. Under this crust, lava continues flowing, forming a tube-shaped passage. When the lava flow stops, the passage can be evacuated by the magma leaving a large-dimension tubular cave. This process of overcrusting is the most common process on Earth but other mechanisms of lava tube formation are based on inflation, in which each layer of cooled lava is lifted by the following lava wave, leading to even larger, more complex cavities [8]. Lava tubes on Earth are common in basaltic shield volcanoes and, by analogy, they are also expected to be common in lunar Maria. In [3], it is shown that differences in planetary parameters (gravity, thickness of the crust, effusion rates, surface temperatures, etc.) could lead to the formation of lunar tubes that could reach hundreds of meters in diameter, be several kilometers long, with volumes of hundreds of millions of cubic meters. Access to lunar lava tubes might be found in some lunar pits, when they represent proper skylights, areas in which the ceiling of a tube has collapsed [9]. Lunar pits exhibit common characteristics, such as circular to oblate outlines, near vertical walls, and a lack of overflow or ejecta on their rims. Over 200 pits have been found on the Moon [10]. [2] described the three deepest and most promising for accessing volcanic subsurface cavities: Marius Hills Pit, Mare Tranquillitatis Pit and Mare Ingenii Pit. However, several pits are not situated in volcanic terrains, but in impact crater melts. In these cases, mechanisms similar to lava tube overcrusting may have led to the formation of other types of subsurface voids in impact settings.

There are several reasons for the interest in these underground features in space exploration and research [11,12]. Subsurface cavities are shielded from radiation, micro-meteorite bombardment, and particle implantation, along with having more stable thermal conditions [13]. From a scientific perspective, this represents a conservative environment with accessible, well preserved lava rock samples, secondary minerals and potential volatiles. Moreover, the shielding also provides a secure place for humans and instruments in the case of long exploration missions or settlements, which could also take advantage of possible water ice trapped in the cave and other mineral resources.

Given the possibilities associated with lava tube exploration, the European Space Agency (ESA) launched a Campaign through its Open Space Innovation Platform (OSIP) for novel ideas (system studies) to address the detection, mapping and exploration of lunar caves on the Moon. These ideas needed to tackle some of the challenges associated with lava pit exploration: power and data distribution inside the caves, robotic exploration systems, science payloads, etc.

Five projects were selected in the OSIP Campaign by ESA [14,15]. Three focus on small-size exploring robots to be deployed inside the lava tubes. The University of Manchester propose a hopping robot, while the University of Würzburg [16] look at a spherical mapping unit, and the German Research Center for Artificial Intelligence [17] propose different-shaped tethered rovers each with different functionalities. The fourth project also addresses exploration of the lava tubes, but using a different approach: a rover operating on the surface and measuring the gravitational field to detect the presence of lava caves. On the other hand, the project presented in this paper (called RoboCrane), focuses on supplying energy from the surface along with a communication link to the surface, for a swarm of rovers deployed inside the lava tubes. Not only does it meet several specific needs underlined by previous studies [18], but also provides the infrastructure necessary for the other three teams selected by the ESA for deployment, power supply, and communication for different cave units.

The proposed system relies on a crane mounted on a Rover, which together make up the surface element (SE) of the mission. Using a crane avoids any unstable terrain around the pit rim as well as preventing wear on wires in a tethered option (in which the wire would be in contact with the irregular skylight edge and walls). This SE is capable of deploying a Head (the Charging Head, or CH) inside the skylight and keeping it suspended close to the bottom of the pit (skylight). This CH has equipment for controlling the deployment and for providing the robots exploring the cave with communications and power. These robots are called Cave Elements (CE). The cable used by the crane for suspending the CH also provides an electrical connection between the SE and the CH. Thus the cable performs a mechanical function – supporting the CH – and an electrical function—powering the equipment inside it. When the CEs are running out of energy, they can approach the CH to be charged from the energy collected by the SE Solar Panel. Given the uncertainties of orography in the pit floor, the CH is equipped with a wireless power charger [19,20], so the only requirement for the robots to be charged is getting close to the CH, which avoids the complexity and problems of chargers based on physical contact in this particular situation. The wireless charge also ensures that energy transfer can begin as soon as the CE is in the vicinity of the CH, which avoids it spending time establishing physical contact between terminals.

Crane design is always a challenging task [21,22]. In this particular case there is not much research focused on cranes for planetary exploration, and none has targeted the specific requirements and conditions explained above. [23] announced the winners of NASA's Lunar delivery challenge (released in 2021), within the framework of the Artemis program. The presence of astronauts on the lunar surface for long periods of time will require deliveries of supplies and equipment to be unloaded once they reach the lunar surface. The winner of this challenge, the LIDS system, relies on an inflatable three-legged movable gantry with a built-in winch, to some extent, similar to the idea proposed in [24]. The same concept is used by the L-tag system, combined with a transportation rover. The Spades proposal is a four-legged movable gantry crane for heavy loads. In all cases, the loads must be delivered within the gantry legs, and it is not possible to hang the load outside that area. Given the large diameter of the skylight, and the unsafe area around the pit rim (roughly 10 m), this approach is not valid for the present project. In the LIDS system, an additional crane rover is proposed for medium loads. Nonetheless, it is based on a Derrick system, which is complex to deploy, bulkier, and normally used for heavier loads than the intended exploration robots [25]. [26] presented a similar structure to the one finally adopted in the Robocrane project. It is based on a truss structure with actuators along its length to give several degrees of movement. This structure is intended to be used in orbital space construction, so the design and behavior is closer to an arm manipulator in zero-gravity conditions rather than a surface crane. Similar structures were proposed in [27] or [28], but always with the premise of in-orbit application, variable geometry for fine positioning of manipulators, etc. In all cases, these structures are always presented as an option with high compact stowage volume, high stiffness and low mass booms, along with high redundancy of actuator function [29,30]. The closest concept to the one proposed in the present paper can be found in [31]. Although this crane is highly versatile and could be even mounted on a rover, it is designed with a reach of 8 m, not even enough to deal with the unstable terrain around the skylight. In addition, it is designed for loads up to 1000 kg, leading to the use of a Derrick system. As previously noted, given the low mass of the exploring rovers, this complex system is not advisable for the current application. As stated in [32], it was not conceived as a traditional crane with the sole purpose of lifting loads, but was also designed for manipulator-type positioning operations, far beyond the requirements of the project

described in this paper, adding complexity without significant benefits. In any case, the demonstration of that crane helps to justify some of the technical decisions made in RoboCrane, such the use of a single cable for deploying the exploring robots.

The CH also behaves as a relay in communication between the exploring robots (CEs) and the surface. The information coming from ground station is received by the SE, sent to the CH, and broadcast inside the cave. CEs can send information to the ground station using the CH and the Crane as relays.

These are the two main objectives of the crane system, but there are two additional potential tasks that it can also do. First, the crane can deploy and retrieve the CEs to and from the lava caves through the pit, meaning simpler designs. This only requires a grappling system to be included in the CH. Second, the CH can be equipped or hold equipment for specific scientific missions, such as sample acquisition, spectrograph analysis, 3D mapping of the pit walls, etc.

The paper is organized as follows. The challenges of Lunar Pit exploration are described in Section 2. The mission description, as defined in the OSIP call and in which the proposed system would be used, is described in Section 3. The System Engineering of RoboCrane project is described in Section 4, including the concept of operations and mission phases, the functional architecture, the system modes and the interfaces. All the subsystems examined are described in Section 5. The ultimate aim of the project, as requested by the ESA, was to develop a parametric tool so the design constraints and input variables could be easily changed and the resulting implementation changes accordingly. The explanations in Section 5 are presented taking this into account, focusing on the general idea and the main design considerations, rather than on specific design values. Section 6 focuses on the aforementioned parametric tool. Section 7 analyzes several design configurations resulting from the parametric tool. This Section 7 also includes some important considerations that can be applied to the mission and RoboCrane project in general. Finally, conclusions are given in Section 8.

2. Challenges of lunar pit exploration

In order to understand the proposed design, it is necessary to explain the main problems facing exploration of lava caves. It is also useful to understand previous approaches to the same or similar problems.

Lunar pit exploration remains one of the most challenging mission scenarios in lunar exploration [18]. There are many topics which need to be assessed to finally achieve feasible exploration missions in these pits and the underlying lava tubes [11,33]. These include robotic concepts for cave access along a vertical wall, navigation and progression inside the caves, science payloads, power, communication, etc.

Various approaches have been proposed for entering a lunar pit [18]. Considering the vertical or overhanging rock walls and the depth of tens of meters, tethered systems have been the most widely studied to date. For example, the mission MoonDiver, proposed recently for the NASA Discovery program, relies on the tethered two-wheeled rover, Axel, developed by JPL [34]. However, the morphology of the pits presents some challenging morphological conditions. The edge of lunar pits are usually not sharp, but they are characterized by a sloping funnel with loose regolith. Any activity along this funnel would create mechanical instabilities in the regolith and underlying loose rock fragments, causing dust avalanches and rockfalls. Any robots or instruments in the vicinity of the wall could be affected by the falling material. Therefore, several approaches which avoid contact with the pit walls have been examined, including cavehoppers, spherical microbots, and flying robots [35–37]. However, none of these solutions would allow the controlled, slow descent needed to scientifically document the pit environment. Instead, a robotic crane solution would allow a controlled descent in the inner part of the pit, without any unnecessary contact with the slope funnel or the pit walls. A crane would be a flexible surface solution for deploying or recovering different types of instruments and exploration units. In addition, communication and the power network inside the cave plays a key role. At the bottom of the skylight, solar energy availability is limited to a few days due to pit depth and wall shadows. Inside the lava tubes, solar energy is never available. For the same reason, there is no direct line of sight between lava tubes and the surface, so communication between exploring robots and the ground station is not a straightforward challenge. According to [18], using a single, bulky robot, capable of easily overcoming obstacles on the floor seems to be ineffective. First, it would not be able to pass through narrow passages [38]. Second, it would be prohibitively expensive to launch due to the mass and volume requirements. Therefore, [18] proposes using a swarm of small robots as a more effective approach. The analysis shows cavehoppers (robots with a hopping system as in [37] for overcoming large obstacles and with wheels for efficient flat-terrain mobility) and tethered wheeled robots (with a tether system for the descent and wheels for flat-terrain mobility) as more effective designs. The crane proposed in this paper would support this mission strategy.

3. Mission description

In this section, the mission will be described in terms of objectives and requirements. It is important to note that given the project design stage, the requirements coming from the ESA are, in many cases, general descriptions or ranges rather than fixed, well-defined limits.

3.1. Scientific objective and mission concept

The scientific objective is the environmental, morphological, and geological study of a vertical lunar pit (skylight) and of the lava tube that might be accessed from the pit bottom, by means of a scientific support system based on a moon surface rover, a deployable crane, and a team of small movable payloads (CE).

3.2. Mission requirements

The main mission objective is the exploration of Moon pyroducts, focusing on the Marius Hill skylight located at 14.091 1N, 303.223 1E. The nominal mission duration shall be 14 days, which equates to roughly half of a synodic lunar period during which the surface around the target cave will be exposed to sunlight.

The system shall be able to advance the estimated 500 m from the landing point to the skylight edge. Also, the system shall conform to the physical constraints imposed by existing launch and transportation systems, namely the upcoming European Large Logistics Lander (EL3).

Based on the initial OSIP requirements, the RoboCrane will be capable of deploying CEs to the floor of the skylight, to a depth of up to 50 m. The rims around the skylight are most probably highly unstable, so they can only be approached safely up to a few meters (around 10 m) from the edge. This is one of the reasons for using a crane-based system, rather than a pure tethered system. In addition, exploration and analysis of the skylight wall is a possibility for the mission, so some distance from the wall may be required to perform tasks related to 3-D mapping, capturing images, etc. .

In the exploration of the cave, the system (i.e. the CEs) must be able to penetrate at least 200 meters into the pyroduct while keeping a constant communication link with the SE.

Because sunlight cannot reach the bottom of the pit, electrical power must be delivered to the CEs via the SE. The power budget of the SE must accommodate the power consumption of both the SE and the CEs. To avoid loss of communication during the charging process, the WPT interface shall be compatible with the simultaneous operation of the communications interface.

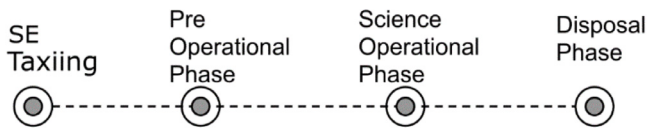

Fig. 1. Mission phases.

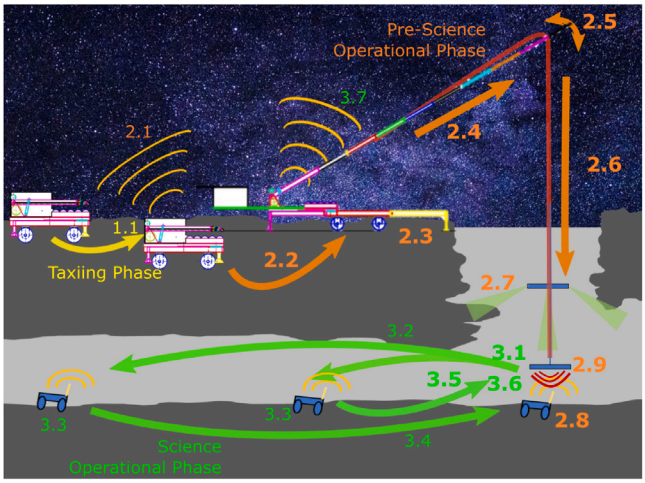

Fig. 2. Scheme of mission phases and concepts of operations. Operation numbering is in Table 1: Taxiing, Pre-science, and Science phases.

4. Systems engineering

In this section, a general description of the mission will be given in terms of phases (concept of operation), based on the mission requirements. Then, the functional architecture will be presented, as a way of providing a general view of the proposed technical solution. Finally, the system modes (dependent on the phases) and the interfaces will explain how the elements are related. This will make it easier to understand the explanation of each subsystem provided in the next section.

The RoboCrane project focuses on the system to route power and data from surface to the lava pit, but it also depicts the system engineering for the different stages from landing site to end of mission. There are three reasons for this: it is a requirement of the OSIP Campaign, the proposed system can help in some of the initial stages and, finally, some parts of the system are defined or affected by these stages. Therefore, in this section, the system engineering for the whole mission is presented.

4.1. Concept of operations

The mission has been designed in order to be executed in four mission phases (see Fig. 1).

A more detailed operation baseline is presented in Table 1, and graphically for phases 1 to 3 in Fig. 2 and phase 4 in Fig. 3 (phase 4).

The mission stages are briefly described within the concept of operations to justify some design decisions presented in the next sections.

Taxiing phase.

Taxiing from lander to marius hill skylight As a Campaign constraint, the Lander will touch down on the lunar surface at an unknown point inside a Landing ellipse with a radius of 500 m. Additionally, this ellipse will be 500 m from the Marius Hill Skylight for safety reasons. That forces the SE and the CEs to travel that distance on their own. Given the size and design of the SE (equipped with a full power subsystem, including batteries and solar panels), it is a reasonable distance. However, it may not be possible for the CEs (i.e.,small-size robots), which are intended to explore the lava pits to a maximum distance of 200 m in a dark environment (i.e. solar panels are not mounted on those robots and their battery capacity and speed may not be sufficient).

To overcome this problem, the SE has a docking area where the exploring robots are stored during the taxi stage. This means increasing the loading capability of the crane, but it alleviates issues with CE design and allows them to be manufactured without large batteries or

Table 1
CRANE mission operational phases, scheduled activities and operation elements.

CRANE mission phase	Schedule activities	Operating element
Taxiing phase	1.Taxiing from landing point to cave pit proximity	SE
Pre science operational phase	2.1. Radio link to Earth	SE
	2.2. Exploration of suitable point for SE leveling	SE
	2.3. SE leveling	SE
	2.4. Unfold the crane	Crane
	2.5. Rotate the crane	Crane
	2.6. Deployment and calibration of Charging Head	Crane
	2.7. Inspect the cave pit to detect obstacles	CH
	2.8. Cave Elements release	CEs
	2.9. Establishment of CH–CE wireless communication	CH–CEs
Science operational phase	3.1. CEs battery charging	CH–CEs
	3.2. CEs taxiing to experiment target location	CEs
	3.3. Execute experiment and data transmission to CH	CEs
	3.4. CEs taxiing to charging head and alignment	CEs
	3.5. SE manages and communicates to CEs their following tasks	CH–CEs
	3.6. CEs battery charging and data transmission	CH–CEs
	3.7. TC/TM/SciData link between Earth and Rover	SE
Disposal phase	4.1. CEs taxiing to Crane CH	CEs
	4.2. Crane CH to lift CEs to SE	CH
	4.3. Crane to be retracted within SE	Crane
	4.4. Disconnection and passivation of all elements	All

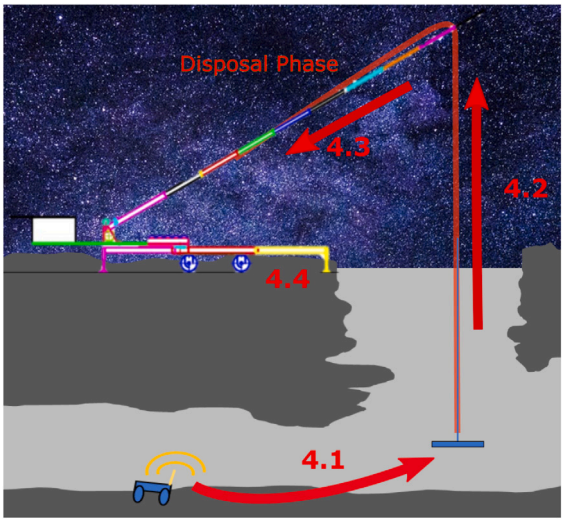

Fig. 3. Scheme of mission phases and concepts of operations. Operation numbering is in Table 1: Disposal phase.

solar panels. Moreover, it will also be an advantage for deployment inside the skylight.

Pre-science operational phase.

Search for a suitable deployment point. The terrain structural performance around the pit rim and its orography is unknown [39]. Pictures of the pit rim show rocks of different sizes, but spatial resolution of the picture limits the minimum observable size (> 1 m). Therefore, preliminary deployment points around the skylight may be chosen during the mission definition, but the SE will need to run onsite checking to ensure the chosen points are valid. The chosen point must ensure that the crane's solar panels receive enough solar irradiation during the full duration of the mission (one lunar day), that the terrain is stable enough to ensure that the crane will not tilt over while deploying the CEs or the CH, and that undetected boulders will not compromise the system. There are more conditions, but they are related to a subsequent stage.

Crane deployment. The crane (see Section 4.1) has a mast which, depending on the final design, may be as long as 25 m. The dimensions of the launch vehicles' cargo holds are shorter than that (e.g. Ariane 5 ECA has a usable volume of 10 x4.5 m in its largest section). In addition, it would be impossible for the crane to taxi from the lander to the skylight over the uneven lunar surface while holding that 25-m mast. Finally, orography and physical characteristics of the regolith make an anchoring/leveling system necessary. Therefore, the crane presents two configurations. One for taxiing and exploring, and the other for crane operation (with outriggers and mast extended). Changing from one configuration to the other is a complex process that requires a well-designed procedure. This procedure is described in Section 5.1.7.

Skylight and pit floor analysis. Once the crane is deployed, the CH is lowered through the skylight to check that the descent is safe for the future deployment of the exploring robots and the CH itself. It also checks the pit floor to assess suitability, both for releasing the CEs and for the charging process when needed. In this latter case, the use of a wireless power charger alleviates issues, as it only needs an area that can be transited by the robot and a reasonable tilt.

There are two options if the descent path or the deployment point in the pit floor are not suitable. One is the crane changing them by changing the mast reach or by rotating it in azimuth. This means that the location of the crane in the lunar surface does not changed. The other is changing from deployment mode to taxi mode and seeking a new deployment point (as described in the Pre-Science Operational Phase).

Exploring robot deployment. One by one, the CEs are deployed inside the lava tubes through the skylight. To do that, the CH is equipped with a hold and release system, which must be capable of releasing and reattaching CEs easily. The SE carrying the CEs is then another advantage, as their location is well defined and their container and orientation can be optimized for the grappling process.

Science phase.

Scientific activities inside the cave. Once all the robots are deployed, the crane will keep the CH inside the pit, suspended over the pit floor at a suitable distance. It will behave as a wireless charging station and as a communication relay. As already explained, inside the caves there is no access to solar light and there is no direct line of sight for controlling the exploring robots from the ground station.

Disposal phase.

Final activities after science phase. At the end of the mission, and in order to minimize waste, the disposal phase will take place. The CEs will be retrieved using the crane. Once they are safely stored in the SE, all the elements of the mission will be safely disconnected and passivated.

4.2. Functional architecture

The ESA Moon mission functional architecture is divided into three different levels of detail:

Level 1: Functional description of the overall system.

Level 2: Functional description of each segment making up the ESA Moon system:

Level 3: Functional definition of the elements/facilities comprising all four segments. Focusing here on the Moon Segment:

- Launch Segment
- Moon Segment:
  - Surface Element (SE).
  - Cave Elements (CEs).
- Ground Segment:
  - Mission Control Center (MCC).
  - Payload Operations and Data subsystem (POYD).
  - Ground Station Network (GSN).
  - Telemetry/Telecommand Gateway (TMTC).
- User Segment:
  - European Space Agency (ESA).
  - Moon Scientific Community.

As a physical implementation of the functional architectures outlined above, the product tree is shown in Fig. 4. The main content of this paper relates to the CRANE subsystem (level 4 and beyond). The CRANE itself is divided into three components: STRUCTURE (ST), CABLE (CA) and HEAD (HE). They are divided again into elements that allow the CRANE subsystem to operate correctly. The individual elements will be described in the subsequent sections of the paper, while here a short description provides a general overview.

The Structure component (ST) is the part of RoboCrane that will remain on the surface of the Moon attached to the rover. The main constituent is the Mast mount (MM) that includes the chassis, the rotating platform, etc. (as explained in Section 4.1), and its main role is ensuring the stability of the SE during deployment and during operation. This stability is monitored and controlled by the Deploy and Control assembly (DC), which also manages cable deployment. Then there is the Mast (MA) itself. Finally for managing all the power demands of the head and to provide an electrical interface between the SE power system and the cable there is the Structure Power Terminal (ST-PT). Communications between the SE, the CH, and CEs is achieved through the Structure Comm Terminal (ST-CT) with the help of the Mast Comm Terminal (Mast-CT) which is powered through the Mast Power Wire (Mast-PW).

The CABLE (CA) is divided into the Power Wire (PW), which distributes electrical power and the Support Wire (SW), which mechanically supports the weight of the CH (and the CE when being deployed).

The HEAD is the part of RoboCrane that interfaces with the CEs. The HEAD is divided into several subsystems. The CH-Power Terminal (CH-PT) takes electrical energy from the power wire and distributes it inside the CH. The RF Subsystem (RS) ensures communication to the CEs and to the main rover structure through the Mast. The wireless subsystem (WS) recharges the CE batteries through a short range wireless power link. The CE Hold and Release (CE-HR) supports the CE during the descent and releases it at the bottom of the pit. Finally the Sensor Package (SP) has a suite of sensors to guide the descent of the crane and a computer to process the data from the sensors to plan the movements and detect abnormal conditions. Finally everything is supported by the Head Structure (HS), which also helps to manage the heat load of the HEAD.

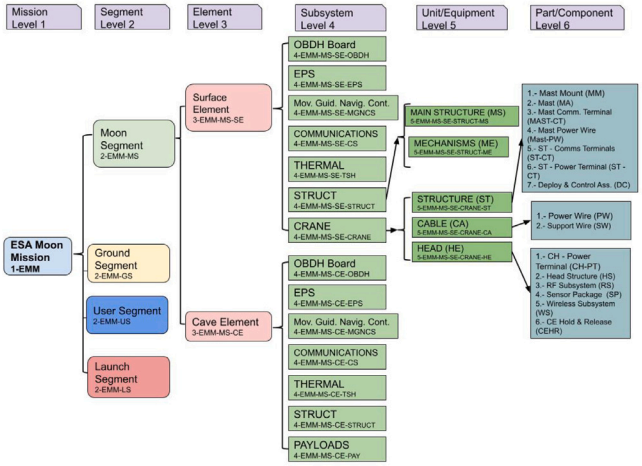

Fig. 4. Product Tree.

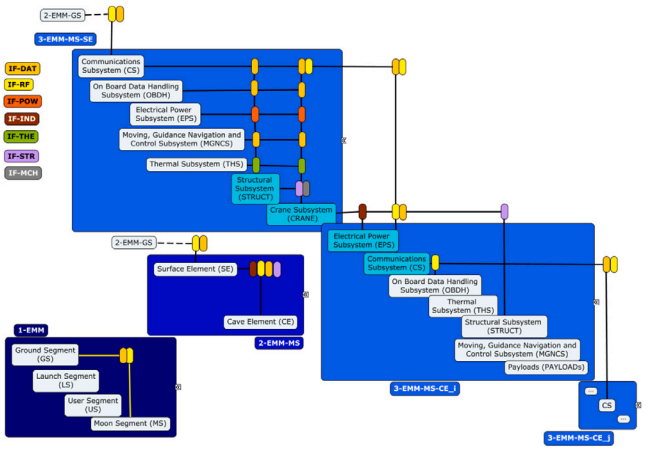

Fig. 5. Map of system interfaces. System levels 2 to 4.

4.3. System modes

In order to accommodate the equipment operations described in the product tree to the phases described in Section 4.1, three system modes have been envisioned. Actually more modes have been defined, such as a safe mode. However, these three modes will suffice to determine the demands in terms of power budget towards the SE power subsystem. The modes are:

- Extending Mode: This mode corresponds to the SE stabilizing itself and deploying the mast.
- Deployment Mode: This mode corresponds to the CH being lowered inside the pit carrying an inactive CE.
- Science Mode: This mode corresponds to the CH being static at the bottom of the pit acting as a communication relay and a battery charge station for the CEs.

In each of the modes the different Elements in the product tree will be active with an appropriate duty cycle so that the RoboCrane system can fulfill its mission.

4.4. Interfaces

The RoboCrane system interfaces, focused on the moon segment, are identified and analyzed. The scope of this interface analysis is to state the interface breakdown at system level up to level 4. Each interface is identified as IF-TYPE-M/N, where IF indicates that it is an interface; TYPE is used to indicate the type of the interface; M for the first interface element, and *N* for the second interface element. The types of interfaces are described in Table 2.

The system elements, categorized as described in the product tree, are associated each other according to the interface map shown in Fig. 5, while each interface is briefly explained in Table 3. As mentioned above, one of the objectives of the RoboCrane system is to provide power and communication capability between the inside and the outside of the lunar cave. This is achieved by means of the radiofrequency IF-RF-3MS-SE/3MS-CE, the data IF-DAT-3MS-SE/3MS-CE, and the inductive IF-IND-3MS-SE/3MS-CE interfaces between the SE and the CEs. Additionally, a mechanical interface (specifically, the structural interface IF-STR-3MS-SE/3MS-CE) will attach the CEs (one at a time) to the CH during the deployment, lowering, and retrieval operations.

Table 2
Types of interfaces.

TYPE	Name	Description
RF	Radio frequency interface	Communication interfaces, which are subdivided into different communication layers (Physical, Data link, etc.)
POW	Power interface	Power transference between two or more elements
IND	Inductive	Inductive power transference between two physically separated elements
THE	Thermal	Interfaces to describe the control and system thermal interaction
STR	Structural	Structural interfaces. These interfaces describe dimensions, mass, envelopes, mounting characteristics, etc.
MCH	Mechanisms	Mechanism interfaces. These interfaces describe deployment mechanisms.

Table 3
Description of interfaces.

IF ID	IF description
Level 2	
IF-RF-2GS/2MS	Radio frequency communication between the surface unit and ground station in X or S-Band.
IF-DAT-2GS/2MS	Data interface to exchange information between GS and SE or CEs. Data class: TM, TC, video, science data
Level 3	
IF-RF-3MS-SE/3MS-CE	Radio frequency communication between the CE and SE
IF-DAT-3MS-SE/3MS-CE	Data interface to exchange information between CE and SE and RoboCrane: Communication protocol between the SE and the CEs which allows the CEs to communicate with Earth. This interface includes the Medium Access Control (MAC) mechanism to coordinate access to the radio channel shared by all the elements within the Cave
IF-IND-3MS-SE/3MS-CE	Power distribution interface between the SE and the CEs through the Crane subsystem. This interface defines how the CEs batteries are charged using the inductive coupling charging interface located in the RoboCrane Head and in the CEs.
IF-STR-3MS-SE/3MS-CE	Mechanical interface between the CH hanging system and CEs, during the CEs descend operation from cave outer pit to cave inner floor.
IF-RF-3GS-XX/3MS-SE	Same as IF-RF-2GS/2MS
IF-DAT-3GS-XX/3MS-SE	Data interface to exchange information between GS and SE. Data class: TM, TC, video, science data
IF-DAT-3GS-XX/3MS-CE	Data interface to exchange information between GS and CEs. Data class: TM, TC, video, science data

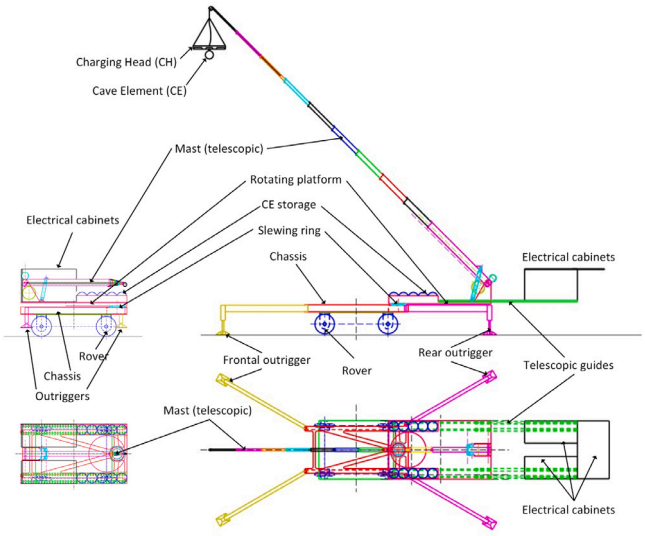

Fig. 6. Crane in taxi mode (left) and deployed mode (right) with the telescopic mast (CE not to scale).

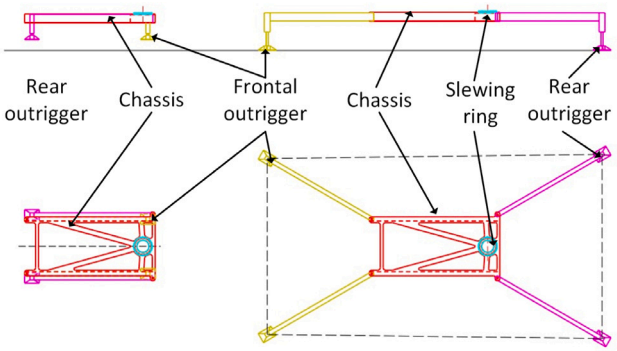

Fig. 7. Main chassis in taxi mode (left) and deployed mode (right).

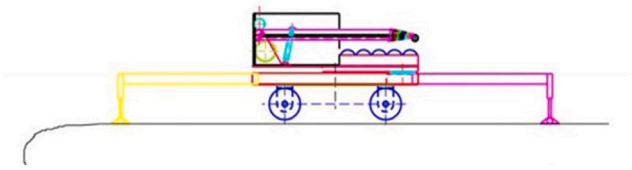

Fig. 8. Crane with the four outriggers deployed and leveling the whole structure. The rover wheels are detached from the lunar surface and the mast is not yet extended.

5. Subsystems description

This section details the main subsystems of the RoboCrane mission. Each subsystem explanation is split into its constituent elements, based on the general description given in Section 4 (which allows allocation of each subsystem and element in the overall design). All design decisions will be justified considering the mission objectives and requirements in Section 3.

5.1. Mechanical subsystem

The objectives for the design of the crane are the SE being able to taxi from lander to lunar pit, being stable when in deployed mode, and providing a data and power link to the CEs in the cave through the CH. It is important to note the main challenge in the crane's mechanical design is achieving stability, given the characteristics of the terrain, the length of the crane and the weight lo lift. Therefore, all the design solutions presented have been developed with stability as the main objective. A schematic of the SE (crane+Rover), in both taxi and deployed mode, is presented in Fig. 6.

5.1.1. Rover

All the elements to provide the crane with taxi capability (motors, gearboxes, wheels, mechanical structure, etc.) are collected together in this element, and they are considered outside the scope of the present project. The main reason is having a crane whose main base design is not subject to the Rover characteristics, so it can be easily adapted in forthcoming stages of the OSIP study (it can be considered as a requirement imposed by the OSIP call). However, two considerations are needed. First, the weight of the Rover (and the position of its overall center of gravity) is important for the stability calculation of the SE (crane+rover). Second, electrical elements which are shared by the Rover and the crane are also used as counterweights, as will be described later. Therefore, although they are also outside the scope, their weight is relevant to the mechanical design.

5.1.2. Mast mount

The Mast Mount Element in the Product Tree is divided into the Main chassis and the Rotating Platform.

5.1.3. Main chassis

The main chassis is shown in Fig. 7. Its purpose is to provide a link between the Rover and the crane, an anchoring point to the rotating platform by means of a slewing ring and, most importantly, leveling the crane during the deployed mode by means of four outriggers. Because it is the link with the Rover, changes to the Rover will mainly affect chassis design, with the rest of the crane elements unaffected. The outriggers are folded during taxi mode (see Fig. 6, left and Fig. 7,left), but once a suitable deployment point is found, they will be deployed in a two-step operation. First, the outriggers are deployed by rotating in azimuth, as shown in Fig. 7, right. The angle can be independently selected for each outrigger, in order to place each of them in the best positions (avoiding boulders, holes, etc.). This also enlarges the stable area. In the second step, the outrigger feet are lowered, also independently, so the crane can be precisely leveled (see Fig. 8), placing the overall center of gravity in the most suitable point inside the stable area.

Given the unknown characteristics of the regolith, presumably made up of loose particles to a considerable depth, the proposed method is more suitable than any other anchoring system. The only foresight to make is designing the stabilizers feet with an area large enough so that the pressure in kept under a safe value. Different methods for outrigger deployment were considered, with this one being the best.

5.1.4. Rotating platform

Above the main chassis, the rotating platform is attached to the chassis by means of a slewing ring. This ring is not centered on the main chassis and the platform. It is instead located on the back side. Once the outriggers are settled, the second stage of the crane deployment process is rotating the platform 180 degrees azimuth (see Fig. 6). This rotation adds some complexity to the deployment process, but due to the aforementioned displacement of the slewing ring, the center of mass of the whole crane is displaced backward, improving stability.

As has been indicated, obtaining an stable crane when the mast is fully extended and loaded is not straightforward, and a specific counterweight is needed in most of the possible scenarios. The rotating platform also holds the electrical cabinets (Fig. 6), which store all the electrical elements common to the crane and the Rover: solar

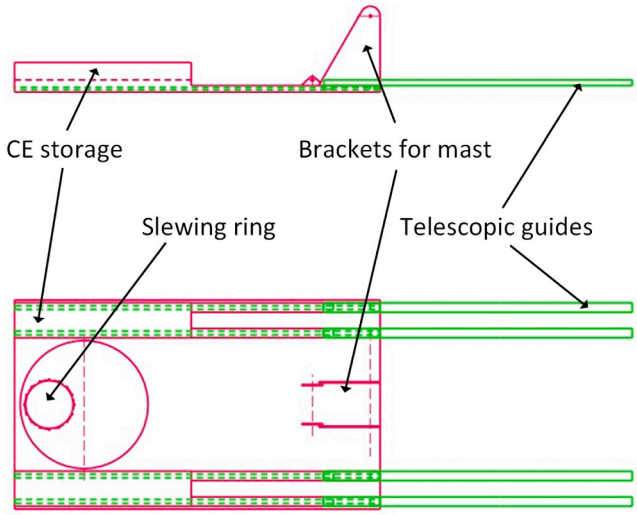

Fig. 9. Rotating platform with the telescopic guides extended.

panels, batteries, power converters, etc. This is to use them as counterweight for the crane, rather than increasing the overall mass of the mission by introducing an additional "dummy load". To enhance the counterbalancing effect, these electrical cabinets are mounted over telescopic guides. When the rotating platform has rotated 180 degrees, the electrical cabinets are moved backwards along these guides (Figs. 6 and 9). These movements may need to be coordinated with the mast extension so that the crane does not overturn backwards due to excessive counterweight. Also, depending on the scenario (final length of the mast, weight of the CEs, etc.), it may not be necessary to use these guides.

The rotating platform also has an area for housing the CEs (see Figs. 6 and 9). In this way, they do not have to taxi from lander to pit, which may be unfeasible for various reasons such as terrain orography, lack of solar panels in the robots, presumably long taxi distance, etc. This also creates a fixed placed for the robots to be picked up during deployment, avoiding problems related to searching for an area, close to the deployment point, for the CEs to wait and be picked up by the crane.

5.1.5. Mast

Three different mast configurations have been examined, all complying with a maximum feasible reach of 25 m and a folded length of 3 m. They (or their containers) are attached to the rotating platform by a pair of brackets, as shown in Fig. 9 for the telescopic mast.

Telescopic mast. This mast is shown in Fig. 10, top and is widely used in conventional mobile cranes. It consists of a series of (normally rectangular) hollow sections such that each section is stored inside the subsequent section, leading to a compact design. When the mast is extended, each section partially slips out of the previous one, keeping a part inside to provide mechanical stiffness. This movement is achieved by a cable, a pair of pulleys in each section, and a winch in the base of the mast. Folding the mast back can be done by lunar gravity or by the action of a second cable and a second winch.

Articulated mast. This is made up of sections consisting of pairs of articulated bars in an x-pattern, as shown in Fig. 10, center. Each section is linked to the following section by joints. This means that if one of the sections changes its relative position (the angle between the x-pattern bars) due to an external action, the same angle is forced onto the other sections. In this case, that external force comes from a linear actuator connected to the first section. Moreover, to give mechanical stability, the mast consists of two of the structures described above, connected in parallel with transverse bars at the joints.

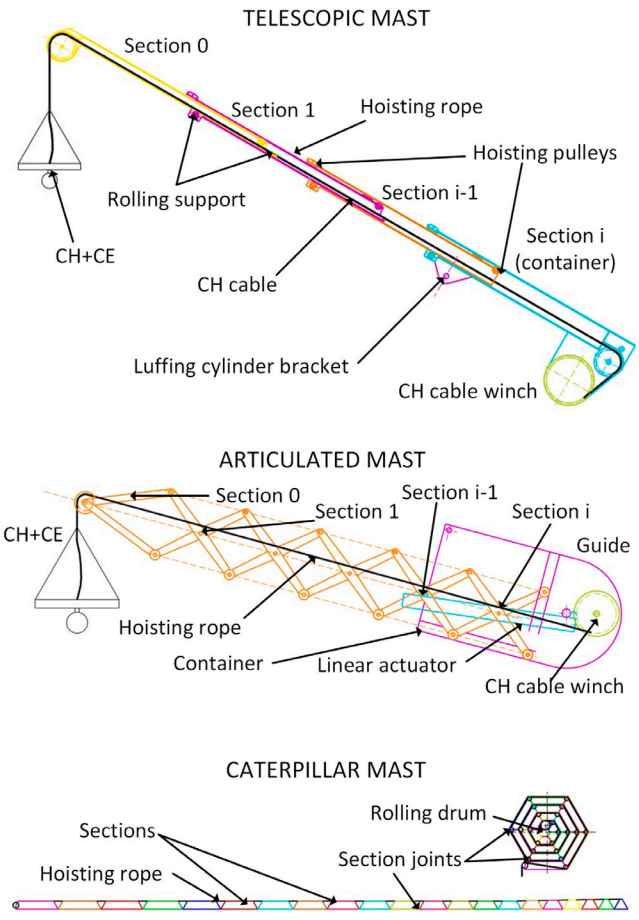

Fig. 10. The three types of mast considered (CE not to scale).

Caterpillar mast. This mast is made up of hollow sections linked by joints, and is quite similar to a cable energy chain. It can be rolled around a rolling core, as shown in Fig. 10,bottom. If this rolling core turns in one direction, it forces the sections to come out through the container output. If the section-joint turn is limited, when the sections come out they will keep a straight shape thanks to the action of gravity. For folding the mast, the rolling drum must turn in the opposite direction. This operation resembles a flexometer.

Mast comparison Table 4 shows the main characteristics of the three masts. Cable Handling indicates the complexity for handling the hoisting cable when folding/unfolding the mast (including length changes) to avoid it getting tangled inside the mast. Pulleys and Joints indicate the quantity there are, considering that they are points of possible failure and increase overall mass. The extension type indicates the kind of relative movement between mast sections. Sliding is worse than rotation given the tendency to get jammed in dusty environments. Dust immunity indicates the inherent protection to dust. The lunar regolith may produce dust clouds that might severely affect the performance of moving elements. Nonetheless, the number of mast folding/unfolding operations is limited to the number of CEs to be deployed plus the initial deployment for exploring the suitability of the descent path. Despite that, these dust clouds will be produced due to the movement of the rover, so dust should be given time to settle down before the crane starts the deployment process. The load/weight ratio represents the ratio between the maximum load mass that can be lifted by the crane and its mass. This last aspect will be discussed more thoroughly in Section 7.

Table 4
Mast comparison.

	Cable handling	Pulleys and joints	Extension type	Dust immunity	Load/weight ratio
Telescopic	Complex	Low	Sliding	Average	Good
Scissor	Complex	High	Rotation	Very Low	Very good
Caterpillar	Simple	Very high	Rotation	Very Low	Average

5.1.6. Charging head

The final design and configuration of the CH will strongly depend on the final shape of the CEs. It will house the wireless power subsystem (described in 5.4.4 and labeled WS), a hold and release mechanism (CE-HR) for deploying the CEs, and sensors included in the sensor package (SP).

The hold and release mechanism is based on an electromagnet. This means that the CEs must include a 3-mm-thick steel plate on their surface. The main advantage is the lack of moving elements, which may be a problem due to loose regolith particles. Moreover, mechanical-based grappling systems may require the CE to include an element to safely grab it (ring, hook, etc.), making the 3-mm steel plate the simplest approach.

The sensors in the CH, as well as its shape and configuration, are also very dependent on the final implementation of the CE and the overall mission. They are discussed Section 5.2.

Apart from that, the CH also includes a Power distribution system, fed from the crane through an electrical wire running in parallel to the mechanical cable. These are described in Section 5.3.

The CH also includes communication equipment for relaying data from the CEs. This is known as the RF Subsystem (RS) and is fully described in Section 5.5. Finally, all this equipment is supported by a structure (HS) that connects the CH to the SW and also serves for thermal management.

5.1.7. Crane deployment

Now all the mechanical elements have been introduced, it is useful to give a brief explanation of how the crane changes from the stowed position to the deployed position. As this is a remote operation, several sensors are required to correctly control the actuators. These will be covered in the following section.

The crane starts as shown in fig6.left. It is important to note that the stowed mast is pointing right. Once the crane is in the selected deployment point with the desired orientation, the outriggers are deployed. This is done by a rotation, as shown in Fig. 7 until the desired angle is reached. Then, the outriggers are lowered until the crane is leveled and stability assured. Then, the rotating platform is rotated 180° (as can be seen in Fig. 6.right, the final orientation of the mast is towards the left). Then, the electrical cabinets are moved back to increase the counterweight effect. The mast is then raised and extended. This is a critical operation which may need the combined movement of electrical cabinets, mast and outriggers. Once this is done, the crane is in position for picking up one exploring robot and deploying it into the skylight. To avoid unwanted oscillations of the load, any mast movement (rotation, inclination, extension) is always performed with the CH (and the exploring robot) close to the mast tip.

5.2. Deploy control and CH sensor package

RoboCrane is conceived to be fully operated from a ground station (i.e. Earth). Consequently, it needs sensors for controlling every movement and action that can be performed by the crane. Several cameras are used to monitor the final position and orientation of the crane in the final deployment point. It is worth noting that current Moon images can only detect boulders and obstacles larger than 1 m; therefore, onsite images will need to be captured to finally assess the selected location. Cameras, load cells and an IMU are used to control outrigger deployment and level the crane. The load cells and the IMU are also used during operation to continually monitor crane stability. Encoders in the rotating platform, the mast and the winch are used to control orientation and the cable release. A Laser Range Finder is used for mast extension.

The CH is also equipped with a sensor package to control the deployment of the exploring robot and its operation as charging station. Specifically, an IMU is used to measure oscillations and rotations. In addition, a LIDAR and a stereo-camera are used to control the descent and detect any possible obstacles.

5.3. Cable

The cable running from the SE to the CH through the mast provides both the support function and the transmission of electricity. It is depicted schematically in Fig. 11. Because it is a critical element, there are redundant pairs of electrical wires (hot and return), so there are two pairs of electrical cables. At system level they are defined as PW. The Support Wire (defined as SW at system level) is depicted in the middle of the arrangement, while the nominal and redundant electrical cables are depicted in yellow and green. The whole set is surrounded by a jacket made from the same material as the SW. This jacket simplifies cable management, treating all the wires as a single wire.

The baseline support wire should be torque free. It is based on fiber designs. Very thin fiber wires (up to 3 mm), made from materials such as Polyester, Technora, Kevlar, Vectran or Zylon have tensile strengths in the range of kilo-newtons. This is much higher than the load represented by the weight of the CH on the moon, the part of the PW that is suspended, and a single hanging CE. However, its compatibility with the environment needs to be tested, particularly resistance to heat and UV radiation. If UV radiation protection is needed, the jacket could be made from another material that protects the core from UV radiation. As a baseline for the model, a 3-mm rope made up of 12×12 strands made from Vectran is selected.

As integral part of the electrical power subsystem, the electrical design of the cable is detailed in Section 6.1.

It is important to note that a significant fraction of the cable will be hanging, so it will impact the design of the crane. This mass is part of the mass that needs to be lifted. So, the bigger the mass of the cable, the smaller the mass allowed for the CEs. The main contributors to cable mass are the power wires. For modeling purposes, the ESCC390101809 from Gore was selected as a good compromise between losses and mass.

The length of the cable is also important for crane operation [40]. Dangling or twisting cables may compromise the mission as it may mean the load crashing against the skylight wall or the floor, uncontrolled deployment of the exploring robots, or the production of high forces in the crane mast, etc. To address this problem, three solutions are considered. First, the cable is composed of different wires and materials, so their different characteristics will provide the cable with some resistance to twisting. As noted previously, a torque free design can also be considered. Second, the CH is equipped with sensors (IMU, stereo-cameras, etc.) to measure oscillations and rotations. Third, any movement of the mast (rotation, elevation, extension) is only done with the CH close to the tip of the mast. In this way, oscillations are limited and easily controllable. If deemed necessary by later stage analysis the CH design could include reaction wheels to counteract them thanks to the gyroscope principle. It is important to note that these mast movements are limited to the deployment and orientation of the crane, so it is feasible to always keep the load close to the mast tip. The exploring robot is always deployed inside the skylight by releasing the cable only, at a reduced speed (in the range of 0.1 m/s). This limitation to vertical movement helps reduce possible oscillations. Obviously, if the deployment point at the bottom of the pit is not suitable, and the mast/crane has to be moved, the cable would be retrieved so the load is again close to the mast tip. This stretches the operation time, but preliminary analysis shows that it is feasible.

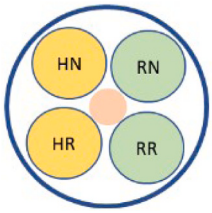

Fig. 11. Cable schematic cross section. (For interpretation of the references to color in this figure legend, the reader is referred to the web version of this article.)

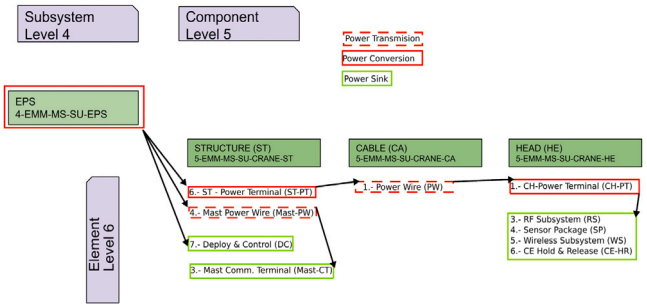

Fig. 12. Power chain.

5.4. Electrical power subsystem

The function of the power subsystem is to distribute power from the SE to the bottom of the pit. It is made up of a wired power distribution from the SE to the CH, described in Section 5.4.2, and a wireless power distribution from the CH to the CEs, described in Section 5.4.4. As shown in Section 4.4, the power transferred to the CEs comes from the Power Subsystem of the SE, which is shared by the crane and Rover. A complete description is given in the following sections.

5.4.1. SE power subsystem

The SE power subsystem is a responsibility of the Rover designers. RoboCrane will be a load to their power system and its power consumption in the different modes will be provided to the Rover designers for adequate sizing. The complete RoboCrane power chain is depicted in Fig. 12. It is divided into power sinks, which are the loads of the system, power conversion stages, which perform energy format transformations, and power transmission, which are mainly wires. The loads will contribute to the power budget by adding power consumption. The power transmission and power conversion stages will contribute to the power budget by adding only losses (while the power provided to their connected loads is only transferred). There are two main contributors to the power demand from the RoboCrane side. The first is HEAD subsystem operation. Its biggest power consumption will be determined by the charging operation of the CEs. The amount of energy that needs to be transferred and the allowed time for doing so will affect the power budget. All the power demanded inside the HEAD is provided through the CH-PT, the Power Wire and the ST-PT. The aggregated losses of those, plus the CEs charging power demand, is part of the power demanded from the 4-EMM-MS-SE-EPS (power subsystem of the SE) by RoboCrane. The other parts are the consumption of the Deploy and Control Mechanism, and the demand of the communications equipment at the tip of the crane, tasked with relaying the information from the CH. This latter unit is supplied through a cable that runs along the mast, at system level labeled Mast-PW. These contributions are modeled in the parametric tool used to represent the system, described in Section 6.

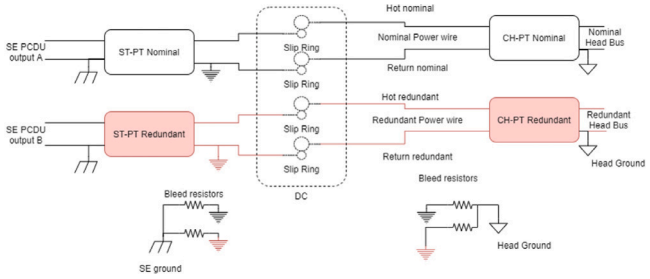

Fig. 13. Schematic of the power distribution between SE and CH.

5.4.2. Wired distribution

The electrical wires running through the cable (see Section 5.3) are an integral, critical part of the system since they will deliver power from the SE to the CH (roughly 50 m apart). Electrical conduction losses through a cable follow the law $P_{loss} = I_{dis}^2 \cdot R_{cable}$, where I_{dis} is the current distributed through the cable. The resistance of the cable R_{cable} is inversely proportional to its section. However, the bigger the section, the greater the mass of the cable. As the cable is part of the suspended mass, it will significantly impact the crane design, and it is advisable to reduce its mass. As the relationship of the losses to the current is quadratic, reducing the current by half will mean reducing the losses to 1/4th. As the distributed power through the cable is $P_{dis} = V_{dis} \cdot I_{dis}$ duplicating V_{dis} reduces I_{dis} to one half. Thus, the same physical wire can carry much more power with lower losses if it operates at a higher voltage. Assuming an SE voltage of 28 V distributing the power to the CH at 50 V or 100 V reduces the losses considerably whilst being compatible with space grade power electronics. Most of the space grade cables, such as the one selected, can withstand voltages in the range of Kilovolts so in that sense there is no problem in running at 100 V.

Operating at a higher voltage than that used in both the SE and the CH means needing a power terminal at each end of the wire. One in the SE (called ST-PT) to boost the voltage distribution, and another in the CH (called CH-PT) that reduces this voltage to a voltage suitable for the equipment in the CH. Nonetheless, the presence of these two converters allows for the galvanic isolation of the electrical wires if isolated topologies are chosen. This galvanic isolation helps to avoid EMI/EMC problems, since all the equipment in the CH will be referred to its local ground. Moreover, this galvanic isolation and the use of bleed resistors will help to address differential voltages that may arise due to the different conditions (in terms of illumination and radiation) on the Moon surface and the bottom of the skylight. Furthermore, the presence of the transformer in the topology helps in voltage scaling.

The cable needs to be retrieved/released during CE deployment by means of a spool. This means that the electrical contact shall be kept for a rotating cable. The power wire will interface to slip rings to allow the cable to be wound in a spool. The ST-PT will interface with the same slip rings to provide power to the cable and thus to the whole wired chain. The overall electrical distribution architecture is described in Fig. 13.

5.4.3. CH power subsystem

The CH power subsystem is responsible for the power distribution of the equipment that is inside the CH. It draws power from the wire through the CH-PT, as shown in Fig. 14.

This equipment includes the communications equipment in the CH (RF subsystem- RS), the Sensor Package (SP)—which helps deploy the crane allowing for a safe descent—, the CE hold and release, and the Wireless Subsystem that recharges the CE batteries.

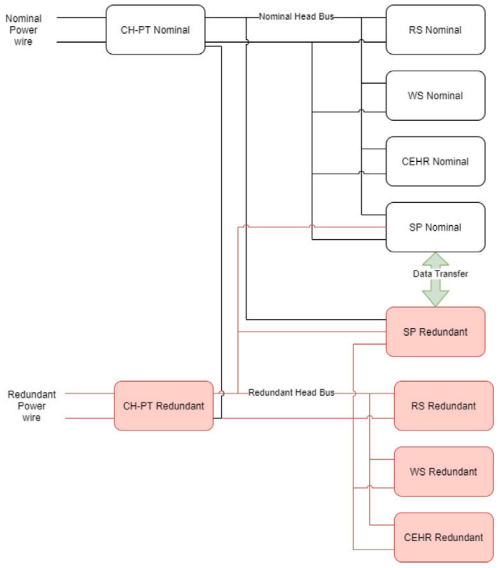

Fig. 14. Schematic of the power distribution inside CH.

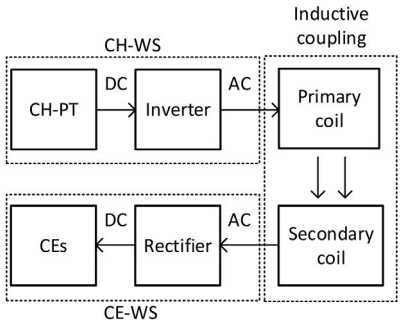

Fig. 15. Schematic of the wireless power subsystem.

5.4.4. *Wireless subsystem power distribution*

The Wireless subsystem (WS) is made up of the transmitter and receiver coils that provide the inductive power link between the CH and each CE as shown in Fig. 15. The wireless power transfer link requires a high frequency AC power flow to work. Since both the CH-PT and the CEs work in DC, an inverter and a rectifier are needed.

At first glance, a contact-based electrical connection between CE and the CH is an easier and more straightforward solution for the CE charging process, however, there are several major disadvantages that justify the use of a more complex WS. The first major problem is the connection time between CH and CE and the need for accurate alignment. The CE has to position itself precisely with respect to the CH so they are able to dock. On top of that, the uncertainties about the pit floor orography have to be taken into account. The required accurate alignment and docking process takes a considerable amount of time, which might easily be longer than the charging time itself. As a result, due to the time added for the docking process and its complexity, this option was rejected.

On the other hand, the need for alignment and proximity is not totally removed by the use of WS but it does add more flexibility. The wireless power link can be designed to transfer power in a range of distances, notably simplifying the positioning process. Providing that the CE is within the charging range of the CH, the charging process will automatically start. It is important to note that the distance affects the inductive coupling between CH and CE, as the longer the distance, the lower the coupling and the lower the maximum power that the charger is able to transfer. If the distance between the CH and the CE means lower coupling than required, the charging process is still possible but at lower power. The simplification of the alignment process significantly reduces the time required for charging, even in cases where minimum coupling is not reached. In these cases, the time saved in alignment compensates for the longer charging time. In addition, the CE can adjust its position during the charging process to try to improve the coupling.

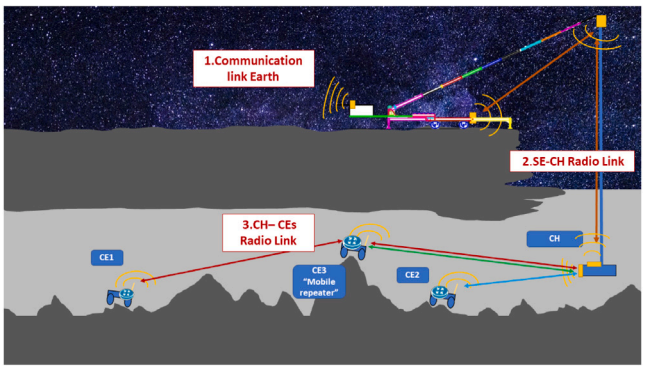

Fig. 16. Schematic of the communications architecture.

The overall time it takes for a single CE to be charged is particularly critical when considering a large number of small CEs, which would need to charge periodically several times throughout the mission. Having the possibility of a fast, periodical charging process reduces the battery requirements for the CE, allowing this solution to work with a wide range of different CE configurations.

Another major advantage of the WS solution is due to the dusty environment on the Moon. In a direct connection solution, the effect of moon dust on the exposed electrical and mechanical connections must be considered. In contrast, the WS allows both the CH and the CE to be enclosed elements which minimizes contamination with moon dust.

Even though more complex WS would be able to charge several CEs at the same time, the proposed solution is designed to charge only one CE at a time, meaning that only one transmitter coil is allocated in the CH and only one CE would demand power from the charger as shown in Fig. 15. This significantly simplifies the power budget calculation and the power sizing on the system. The effect on the power budget is reflected on the tool used to calculate the budgets described in Section 6.

5.4.5. *CE battery charger*

The CE battery charger comprises the different elements necessary to charge the battery of each CE. It is implemented in each CE and controls the power flow of the charging process. It is made up of a Battery Management System (BMS) that charges the batteries and distributes the power inside the CEs. The power flow control in each CE is necessary because, without it, the amount of power from CH to CE during charging would largely depend on the distance between them. This may be a problem due to uncertainty about the surface of the pit. This system will be the responsibility of the CE designer.

5.5. *Communication subsystem*

The function of the communication subsystem is to support the control of the mission from Earth, send real time housekeeping data and return scientific data. The SE will be able to communicate simultaneously with all the deployed CEs by means of an omni-directional, continuously available radio link. Thus, the WS shall not interfere with the communication subsystem in the CH. The architecture of the communication subsystem is composed of three elements Fig. 16:

- Communication link between the SE and the Earth. At the time of writing this paper, space agencies and their industrial partners are developing different activities to deploy a communication network able to provide constant connectivity between the Moon and Ground Control on Earth. This mission could benefit from this future service. This element is out of the scope of this work.
- SE-CH link. This link establishes the communication between the SE and the CH. This link can be made using a wireless link or a communication cable. A analysis of both alternatives is provided in the subsequent section and the wired solution was rejected due to the high mass of the communication cable which would significantly reduce the available mass that could be lifted by the crane (i.e. the CE).
- CH–CE radio link. A radio link will be established between the CH and all the CEs through an IEEE 802.11 protocol. In addition, any of the CEs can act as "mobile" access points that ensure direct Line-Of-Sight (LOS). This set-up allows multi-robot coordination [41,42].

5.5.1. Communication link between SE and CH

Wireless link SE-CH. This solution consists of establishing full duplex, point to point connection between the SE-CT and the RF equipment inside the CH (RS) through a regenerative repeater, included in the tip of the mast, with view of both SE and CH. This element is known as the Mast Comm Terminal (Mast-CT). This repeater shall cover a distance equal to the depth of the pit (around 50 m) with line-of-sight (LOS) so relatively low transmitted power is needed (10 mW). The antennas do not need specific pointing and they are fixed as long as the angle of mast can be kept in a limited range. This solution would require deploying a power cable through the mast to supply power to the regenerative repeater (Mast-CT) located in the mast tip. The mass of each of the communication terminals will be around 200 g, taking cubesat technology as a design basis. All the communication equipment (ST-CT, Mast-CT and RS) will be redundant, as it is the only communication path between the surface and the cave, and it is considered as a critical element.

Cable link. The use of a cable link between the SE and CH was also analyzed as an alternative to the wireless link. This solution involves a physical cable which would be deployed together with the power cable.

For the wired solutions different current and near-term available space qualified standards or technologies were identified:

- MIL-STD-1553. It is one of the first communication data bus standards for transmission of digital data between subsystems over a common set of wires, issued in 1973. Its main advantages are high reliability and long historical use in military and aerospace applications. Its main disadvantage is a very limited data rate (1 Mbps maximum).
- SpaceWire. It is the result of a collaboration between ESA, NASA, the European space industry and academia. Its definition is part of the ECSS standards (ECSS-E-ST-50-12C) and it has been used in several ESA, NASA, JAXA and Roscosmos missions. It is a point-to-point network where each node is connected to a router. Cable length is in the range of 10 m for regular configurations and is its main disadvantage.
- SpaceFibre. It is a standard for very high-speed links. Its definition is also part of the ECSS standards (ECSS-E-ST-50-11C) and was developed as the successor to the SpaceWire, improving data rates up to 5 Gbps. It is not a mature technology but several activities to develop equipment for this standard are ongoing supported by ESA.
- Ethernet. It is a widely used architecture for terrestrial applications. In recent years, the need for higher speed links on board satellites has made Ethernet a good candidate and several efforts have been made to adapt this architecture to space constraints. One recent attempt is SEPHY, funded by the European Commission to try to develop a radiation hardened Ethernet transceiver to meet long cable length (100 m) and high data rates (100 Mbps). It is not a mature technology and commercial components are not yet available.

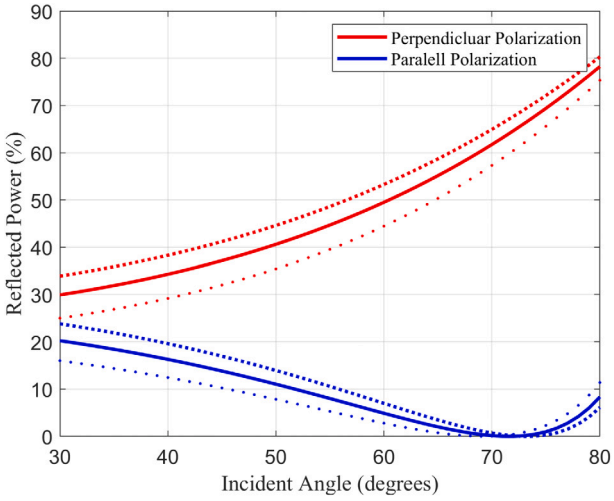

Fig. 17. Estimated reflected power of a single echo inside a lava tube for different relative permittivities (·, $\epsilon_r = 7$; -, $\epsilon_r = 9$; ·· $\epsilon_r = 11$).

In conclusion, the existing standards (MIL-STD-1553 and SpaceWire) have some disadvantages that prevent them from being used in this mission. The most promising options are the near-term available options (SpaceFibre [43] and Ethernet/SEPHY) but none of them has space heritage yet. As already noted, wired solutions were ultimately rejected due to their impact on the mass budget and the available mass that could be lifted by the crane.

5.5.2. CH-CE radio link

Channel model inside cave. Radio signal propagation in a tunnel exhibits distinct near and far regions with quite different characteristics [44]. This behavior is represented as a two-slope model, where a break point characterizes the transition between the two zones. The location of the break point strongly depends on frequency, antenna position, and the tunnel's maximum transversal dimension (a). The break point is at a distance $Z_{bp} = a^2/\lambda$, where λ is the signal wavelength in free space.

The near region path loss slope is modeled as free space path loss. In the far region, the waveguide effect appears with few lower order modes and the path loss slope is reduced significantly. In [45], measurements performed in a 16 m wide, 7 m high road tunnel at the carrier frequency of 2.1 GHz show a break point at about 300 m. In view of these previous results, the communication link between the CH and the CEs will be performed in the near region. The free space model is suitable for the LOS condition. Under non-LOS (NLOS) conditions, in the near region, only reflection and diffraction contribute to the received signal strength and the propagation losses increase considerably. To keep the SE–CE continuously available, some CEs will act as relays. To evaluate the losses in NLOS, a one-echo model has been studied. For caves up to 10 m below the lunar surface, the propagation can be modeled as a ray that impinges on a planar interface between vacuum and a lunar regolith (of a relative permittivity between 7 and 11 and a negligible conductivity [46]). Fig. 17 shows the reflected power for different relative permittivities, depending on the angle and the polarization. These results are frequency independent because of the negligible conductivity. It is estimated that the reflected wave could be attenuated by between 70% and 90%.

However, 10 m below the lunar surface regolith density is expected to be greater, so total reflection is expected.

Additional losses must also be added due to surface roughness. To model these losses, the exact tube shape and the exact position of the CE must be known. This is outside the scope of this study.

The communication protocol, like Wi-Fi, inside the cave shall take into account a multipath scenario.

Radio frequency subsystem (RS). The Radio Frequency Subsystem, located in the CH, will be composed of a transceiver (acting as access point) and a set of antennas that allow a MIMO configuration. The antennas do not need specific pointing, so monopole or patch antennas could be used.

Considering the distances inside the cave and the expected data rates, a Wireless Local Area Network (WLAN), based on the IEEE 802.11 standards (popularly known as Wi-Fi), is the most promising alternative, providing high data rates with low power consumption and low latency. WLAN technologies were designed for indoor environments with multipath and they implement features to make communication robust to these phenomena. They take advantage of Orthogonal Frequency Division Multiplexing (OFDM), Orthogonal Frequency Division Multiple Access (OFDMA) and Multiple Input Multiple Output (MIMO) techniques to provide multiuser access to the channel. Several 802.11 standard variants exist with different characteristics such as frequency ranges (from 54MHz to 60 GHz), data rates (from 2Mbps to more than 1Gbps), maximum distances, channel bandwidths (from 1MHz to 160MHz), modulations and codification schemes (from BPSK to 1024-QAM), etc. The best options to consider for this mission are 802.11ax and 802.11ah. 802.11ah provides narrowband communication while 802.11ax provides very high throughput. The two protocols are very different from each other but they both offer good reasons for consideration since they can fulfill the communication trade-offs in different manners.

802.11ax can set a different modulation and codification scheme (MCS) for each agent. Considering the cave scenario, this is another strong point of the standard. This flexibility opens the door to different options. For example, the link budget can be designed to provide each user with the coverage required to obtain the necessary throughput at the prescribed distance of 200 m from the CH but allowing even further penetration with a reduced data rate, still sufficient to operate the CEs in a reduced functionality scenario.

The main advantage of 802.11ah lies in the lower frequency used, below 1 GHz, which accommodates long range requirements or equivalently reduced needs of transmission power, as well as improved obstacle penetration, at the expense of available throughput. It also allows lower channel bandwidth (1 MHz), which reduces link budget needs for low-data-rate but large-range-requirement scenarios(> 200 m).

A similar communications architecture was developed in ESA's CAVES training programme [47], and it was able to establish a stable network inside the cave over a distance of 900 m.

5.6. Thermal subsystem

There will be a very large range of lunar surface temperatures around the pit rim, as on the rest of the lunar surface. However, there is still notable uncertainty about the thermal environment inside the skylight and the lava pits [48].

A first approach to the RoboCrane thermal concept will consider the worst-case thermal variability and uncertainty, so that the components, whose temperatures should be within the range 243K to 348 K, will be insulated as much as possible by means of MLI-covered containers. Components for RoboCrane are allocated in 4 different thermal boxes: boxes 1 and 2 on the Rover, box 3 on the end of the mast, and box 4 on the CH. Each box will be warmed with their corresponding power dissipation according to power budgets.

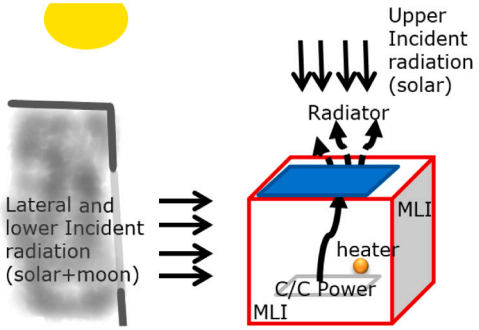

Fig. 18. Thermal model of each box based on one node.

A thermal model with a unique thermal node is provided for each box in order to have a first approach to the level of temperature (see Fig. 18). Thermal boxes are covered by MLI blankets except the upper surface where a radiative surface is placed. Therefore, Dissipation from RoboCrane boxes is radiated upwards. Values for the optical properties will be selected to maintain inner temperatures inside the required ranges, according to component specifications. Holes and access for cameras and cables will be available through the MLI. External coatings for boxes, structural parts and wires would be white paint or covering by OSR.

Estimations for the temperatures of boxes are provided for the crane deployment, skylight exploration, and CE deployment stages of the mission (i.e. when the crane is operative). Moon and solar radiation are considered for bottom and lateral box faces and only solar radiation for upper box faces. The thermal temperatures of the south walls of the lava pit are used as thermal boundaries inside the cave as they are moderate enough for the descent [48]. All temperature calculations are included in the system parametric tool, and the results are presented in Section 7.

6. System budgets (parametric tool)

In this section, the parametric tool for calculating the system budgets will be introduced. First giving the reasons for not giving a final fixed design, but rather a parametric tool that can dynamically calculate them according to variable inputs. Then, the general structure of this tool and the way it is operated will be described.

The OSIP campaign regarding Lunar Caves aimed to tackle several challenges. RoboCrane aims to provide a communication access point and energy supply to the CEs, as well as a safe way to deploy the CEs. But it is not tasked to design either the CEs or the Rover. Moreover, a high degree of flexibility is needed to adapt to different scenarios. These scenarios include skylights situated in different lunar coordinates, different lander requirements, different Rovers, and a variety of CEs. Ultimately, the Rover design and the conditions of the terrain near the skylight will determine the required crane reach. At the same time, the desired crane reach together with the SE and counterweight mass will determine the maximum mass allowed for the CEs. As the design space involves many different parameters, the RoboCrane team was tasked with developing a parametric tool to address the feasibility of the different designs. The objective of this parametric tool is to obtain representative Mass and Power budgets for the designs.

In order to evaluate these different designs, a Model Based Systems Engineering (MBSE) approach was followed in order to have a parametric evaluation of the design. A model for each of the elements in the product tree was created in a Microsoft Excel spreadsheet. Microsoft Excel was used instead of more sophisticated tools due to its widespread adoption. The models will keep track of the mass and power consumption of the elements. The complexity of each of the models varies significantly. Some models are very simple, such as the Sensor

Package (SP) model. In this case it is just a collection of the mass and power consumption of different equipment. Other models, such as the different masts, are very complicated and depend on the reach, the mast design, the mass to be lifted, etc. In these cases, the model performs all the calculations for a feasible design (stiffness, bending efforts, etc.). Other complex models, such as the Wireless Power Transfer (WPT) system or the Communication system, also rely on the number of CEs (apart from other parameters). These spreadsheets are connected so the impact of one subsystem on another is properly reflected. For example, the power consumption of the WPT depends on the energy requirements of the CEs and how many there are. The power demand of the WPT is one of the main drivers for the power transferred through the power cable, which in turn affects the mass and losses of the cable, and then the maximum CE mass that can be lifted by the crane without tipping over.

All the masses and power consumption per operation mode are collected together in the Mass and Power Budgets. These were generated following a bottom up approach, thus aggregating the masses and power consumption of the lower levels of the product tree. These spreadsheets allow for analysis of the individual impact of each of the subsystems in the different budgets, with the appropriate margins. This information is very useful for optimizing the system. For example, it led to the decision of performing the communications between the CH and the SE through RF links instead of a communication cable as was first envisioned.

All the information, including the main design parameters, are gathered in a central spreadsheet. This allows variation of the design parameters, for example the desired reach. It flows the data down to the different individual models that make the appropriate calculations. Then the information flows up to the budgets and back to the central spreadsheet. This provides easy visualization of the calculated parameters that allow rapid evaluation of the feasibility of the design. One of the main calculations performed is the maximum mass that a CE may have. This includes the WPT system part receiving the energy from the CH, the mechanical interface with the hold and release system and the compatible communications equipment. This leaves the CE designers a limit on the mass to refine their design. If they claim that they need more mass, the tool allows for rapid analysis of the solution (for example, reducing the reach or increasing the mass of the counterweight). It also serves to calculate how many CEs can be deployed for exploring the interior of the cave. For simplification, it will be assumed that all the CEs are equal. An example of the usage and capabilities of this tool are shown in Section 7.

6.1. Element calculation example: CABLE calculation

The full model describing the system is too long to include in a paper. In addition, the complexity of the different models for the Component Level of the product tree varies widely. One simple example is the CABLE (CA). This is a Level 5 element which is modeled after the Power Wire (PW) and Support Wire (SW). For the SW, the designer can choose between several commercial synthetic ropes, all of which have a much higher tensile resistance than needed and can withstand extreme temperatures. Therefore, calculations are straightforward here. The final mass will depend on the desired reach and the depth of the pit. However, there will be an influence of the mast design. The PW is modeled after commercial space power wires. The length is of course the same as in the SW, and thus is affected by the same design choices. However, the PW has also an influence on the power budget. The model includes the Ohmic losses. The head will demand power through the PW. Precisely to minimize these losses, the power wire will be running at a voltage, V_{dis}, higher than the HEAD and the rover voltages. The power demand from the head will draw a current from the wire equal to:

$$I_{dis} = P_{head}/V_{dis} \tag{1}$$

This current will generate losses on the cable of value:

$$P_{loss\_wire} = I_{dis} \cdot {R_{cable}}^2 \tag{2}$$

where R_{cable} is the product of the length of the cable and the vendor specification of the resistance per meter. These losses will add to the demand of the HEAD and then to the demand of the rover, which in turn will influence the power budget of the rover. The power budget also takes into account the losses in the conversion stages (CH-PT, ST-PT). The first task of the designer will be to select a wire. Then the designer needs to choose V_{dis}. Then the mass and losses are calculated from the reach and depth specifications and the power budget. The system will let the designer evaluate what would be better, if choosing a thinner, lighter wire with higher R_{cable} or a heavier solution with less losses. The former will be better if the HEAD power demand is small while the latter will be better if the power demand is significant. Examples of these trade-offs, interactions, and calculations are general to all the system elements. Certain elements, especially those related to mechanical design, such as the Mast (MA), mean complex calculations in which the constitutive parts are fully calculated and assessed in terms of size, applied torques and forces, resulting bending, etc.

7. Results

In order to illustrate the capabilities of the modeling tool presented in the previous section, two scenarios will be assessed. These are the most representative from all of the scenarios calculated with the tool, according to the outcomes from ESA assessment. Each scenario will also consider two out of the three possible crane masts. Once calculated, comparing them will allow determination of trade-offs, bottlenecks and aspects in which additional work is required once the mission requirements are refined.

Both will be based on the following assumptions:

- Cave depth 50 m
- Rover mass 410 kg
- Crane structure fixed mass 70 kg
- Crane counterweight mass 80 kg
- Cave element energy to recharge 156 Wh
- Cave element time to recharge 25 min

With these assumptions, two desired crane reaches will be evaluated. In the "Long" Scenario the crane would have a reach of 25 m. For the "Short" scenario, the desired reach will be 12 m. Two mast designs will be evaluated, articulated and telescopic. The results of the analysis can be seen in Tables 5 and 6. Table 5 shows that for the Long scenario, the CE mass that can be lifted by the crane (mass available single CE) is very low, around 3 kg. Nonetheless, this allows the SE to transport more CEs (available mass for CE/mass available single CE). This would theoretically allow deployment of a large swarm of CEs for exploring the lava tube. However, according to Table 6, with 5 CEs the duty cycle of the WS is around 80%. This means that around 80% of the time a CE is being recharged. Since no more than one CE can be recharged at the same time, this means the others may need to wait, which could be present a risk to CE survival capability. Thus, careful planning of operations (charging queue) will be needed. The duty cycle of the WS is then the limiting factor for the number of CEs. Regarding the datarate with 5 CEs the RoboCrane will need around 300 Mbps. In the Long scenario, as the articulated mast is lighter, the maximum available mass for CEs is larger. Also, a lighter mast means that the overall center of gravity of the SE is farther from the front, allowing the crane to lift slightly heavier CEs.

This situation changes when the reach of the crane is reduced to 12 m (Short scenario). In this case, the mass of a single CE can be increased to values around 30 kg, which represents a significant improvement in comparison to the Long scenario. A heavier CE may represent more instruments and capabilities than a smaller one. As

Table 5
Mass analysis result.

Scenario	Mast	Crane Mass (kg)	Suspended Mass (kg)	Mass available single CE (kg)	Available mass for CE (kg)
Long	Telescopic	203.12	17.37	2.27	51.7
Long	Articulated	171.13	17.37	3.81	93.68
Short	Telescopic	186.9	18.74	30.33	68
Short	Articulated	165.33	18.74	30.67	89.67

Table 6
Datarate and WPT duty cycle analysis result.

Scenario	Mast	Number of Cave elements	WPT duty cycle (%)	Datarate (Mbps)
Long	Telescopic	5	78,4	331.82
Long	Articulated	5	78,4	331.82
Short	Telescopic	2	13.4	132.7
Short	Articulated	2	13,4	137.7

Table 7
System mode and duty cycles.

Element	Extending	Deployment	Science
Mast-CT	100%	100%	100%
ST-CT	100%	100%	100%
DC	95%	35%	10%
SP	100%	100%	100%
RS	100%	100%	100%
WS	0%	0%	78.4%
CE-HR	0%	1%	0%

the total mission mass is the same in both scenarios, the SE will only be able to transport two CEs. This means that the WPT duty cycle is considerably lower (13%); therefore, with a simpler charging planning both CEs could be recharged without having one to wait for the other to finish. Fewer CEs also reduces the datarate needs.

The tool also calculates the power, mass, link and data budgets. For the power budget, the duty cycles for the power sinks are needed. Losses in the power conversion and transmission elements such as the power wire are calculated following the power chain described in Section 6.1 and added to the final power budget. Some of the duty cycles such as the Wireless Power System (WS) are automatically calculated by the tool since they depend on design parameters such as the number of CEs. Others are a design input and can be tailored to different scenarios. The ones used in the example are shown in Table 7.

All the communication equipment is always on with a duty cycle of 100%. The DC subsystem (which includes all the elements required for the crane to operate, such as motors) will fully work while balancing the crane and extending the mast and then it will only be used for lowering the CEs to the bottom of the pit. In this case, the movements of the crane were divided into mast extension, mast rotation and head elevation. The energy required and the power allocated for performing the movements in an allowed time (a design input) will be calculated. In each of the modes, a different percentage of the movements will be carried out. For example, in Science mode no mast extension movements will be performed and small elevation and rotation movements are foreseen, hence its low duty cycle. However, extending the mast, in Extending mode, the duty cycle of the DC is 95%. The total average power demand for this example is shown in Table 8 (for the Long Scenario and the telescopic mast), where the typical 20% margin due to the low maturity of the equipment has been accounted for. The figures can vary if the chosen equipment for implementing the elements is different, if the CE energy or mass vary, if more time for the movements is allowed, etc. This is just an example of how the tool allows the power budget to be calculated. Depending on the Rover design, the power demand represented by RoboCrane (payload of the Rover) or other Rover requirements, such as the power needed to traverse, will drive the Rover design regarding the power subsystem. However, this is a task for the Rover designers that was outside the scope of this paper and the study performed. This power budget is also used to size the radiating surfaces of the thermal model described in Section 5.6.

Table 8
Peak and average power consumption per mode.

Mode	Extending	Deployment	Science
Peak power (W)	986.9	1155	534
Average power (W)	940.5	258	219

Table 9
Temperature results of the four thermal boxes for critical hot and cold cases.

Thermal box	Temperature in hot case [K]	Temperature in cold case [K]
Box 1 and 2 outside the cave	322	242
Box 3 outside the cave	342	265
Box 4 outside the cave	340	243
Box 3 inside the cave	328	243

Regarding the mass budget, the mass of the individual elements is calculated and added together, with a 20% margin to form the total mass of 203.12 kg shown in Table 5. One of the main contributors to the mass budget is the mast. The tool automatically calculates its mass based on the desired mast design and reach. With the telescopic design, described in Section 5.1, allowing for a maximum folded length of 3.4 m, the mast is divided into 15 sections having a total mass of 59.66 kg. The total extended length is 33.75 m which serves to surpass the 25 m reach with a 10 degree elevation angle. It is important to remember that to enhance stability, the mast is extended from the back of the rotating platform, so it has to surpass the length of the SE to have an effective reach of 25 m (or 12 m). It is also important that the electrical cabinets are moved back to enhance their counterweight effect. This, along with the low mass of the exploring robots, ensures that the single-mast crane will be stable under the conditions imposed on the mission.

Although it is out of the scope of this paper, the mass and length of the mast indicates that during the test of any model under Earth gravity, it may collapse. Therefore, it will be essential to use gravity compensation system, like those used when testing the deployment of solar panels [49,50], antennas [51] or other elements [52].

The tool allows for rapid iteration over several designs, helping designers to establish various trade-offs. It also serves to identify the main contributors to the budgets and the design drivers. As mentioned in Section 5.5, a wired communication was evaluated and rejected because the tool showed that the main contributor to the mass of the cable was the communications wire. Several bottle-necks and design drivers are also identified through using the tool. For example in Science mode, the biggest power requirement comes from the energy that needs to be transferred to the CEs. If more time is allowed for the transfer, the peak power required will be smaller. However, this means that the CEs will spend less time performing science operations and more time recharging, which will also limit the number of CEs that can be serviced.

Finally, the thermal results are shown (see Table 9), specifically the temperatures of the 4 thermal boxes for critical hot and cold cases, inside and outside the cave, and including 20-K-margin. All are within the required range.

Using the tool, a wide design space with many parameters can be easily explored. Although several simplifications have been made, the tool suffices for early stages of the design.

8. Conclusions

This paper presents the preliminary design of RoboCrane as an outcome of the Lunar Caves OSIP study. It identifies design parameters

for a crane designed to be mounted on a Rover (conforming the SE) able to reach a distance between 5 and 20 m whilst also being capable of lowering low-mass robots designed to explore the caves (the CEs). It also presents several design considerations to achieve a stable crane with a long reach, such as moving the electrical cabinets back to increase their counterbalancing effect. The crane will also serve as a communications access point so the CEs can receive orders from the ground and send information back to Earth. It will provide a wireless power transfer system for recharging the CE batteries. At the system level, the mission phases, system modes and system decomposition have been identified and evaluated. The interest and validity of the proposed design is built on having been selected by the ESA for the second stage of the OSIP call, along with another proposal, so both were merged in the CDF study leading to a final valid preliminary implementation.

All the system design information is stored in a Microsoft Excel MBSE tool that allows for rapid iterations of the design. The tool provides the mass, power, link and data budgets needed. It is by no means intended to be used as a final design but rather as a method to rapidly evaluate different design options. Although simplified it is accurate enough to identify the trade-offs and design drivers.

The tool also helps system level decision making, such as the removal of the communications wire, and helps to identify the places where optimization is needed. For example if a crane reach in the order of 20 m is needed and the mass of the CEs is greater than 10 kg, the mass that the structure and the counterweight that RoboCrane requires would make it advisable to integrate it with the rover structure rather than design it as a structure to be mounted on top of an existing rover. However, if smaller reaches are needed it would be feasible to mounted it on the rover as originally designed. The boundaries of these solutions would require precise analysis outside the scope of the original activity and this paper.

The tool is flexible enough so it can be used for other designs. For example, it can be tailored to a different mechanical configuration than that described in Section 5.1 so bigger CEs could be managed at the cost of having fewer degrees of freedom (i.e: less rotation capabilities, a single CE attached to the HEAD from the beginning of the mission). The equipment and the operation modes can be changed to perform scientific studies of the walls or the pits. In fact a version of this tool has been used in a CDF study in the ESA together with the DAEDALUS team from the original Lunar Caves campaign.

Declaration of competing interest

The authors declare that they have no known competing financial interests or personal relationships that could have appeared to influence the work reported in this paper.

Acknowledgment

This work was supported in part by the Spanish Government under the Project MCIU-19-RTI2018-099682-A-I00 and by ESA, Spain under ESA CONTRACT No 4000130860/20/NL/GLC.

References

[1] J. Haruyama, K. Hioki, M. Shirao, T. Morota, H. Hiesinger, C. van der Bogert, H. Miyamoto, A. Iwasaki, Y. Yokota, M. Ohtake, T. Matsunaga, S. Hara, S. Nakanotani, C. Pieters, Possible lunar lava tube skylight observed by SELENE cameras, Geophys. Res. Lett. - Geophys. Res. Lett. 36 (2009).

[2] M.S. Robinson, J.W. Ashley, A.K. Boyd, R.V. Wagner, E.J. Speyerer, B.R. Hawke, H. Hiesinger, C.H.v.d. Bogert, Confirmation of sublunarean voids and thin layering in mare deposits, Planet. Space Sci. 69 (1) (2012) 18–27.

[3] F. Sauro, R. Pozzobon, M. Massironi, P. De Berardinis, T. Santagata, J. De Waele, Lava tubes on earth, moon and mars: A review on their size and morphology revealed by comparative planetology, Earth-Sci. Rev. 103288 (2020).

[4] V. Oberbeck, On the origin of lunar sinuous rilles, Mod. Geol. 1 (1969) 75–80.

[5] R. Greeley, Lava tubes and channels in the lunar marius hills, Moon 3 (3) (1971) 289–314.

[6] D. Cruikshank, C. Wood, Lunar rilles and hawaiian volcanic features: Possible analogues, Moon 3 (4) (1972) 412–447.

[7] D. Peterson, R. Holcomb, R. Tilling, R. Christiansen, Development of lava tubes in the light of observations at mauna ulu, kilauea volcano, hawaii, Bull. Volcanol. 56 (5) (1994) 343–360.

[8] S. Kempe, Volcanic rock caves, in: W.B. White, D.C. Culver (Eds.), Encyclopedia of Caves (Second Edition), second ed., Academic Press, Amsterdam, 2012, pp. 865–873.

[9] J. Haruyama, T. Morota, S. Kobayashi, S. Sawai, P.G. Lucey, M. Shirao, M. Nishino, Lunar holes and lava tubes as resources for lunar science and exploration, Moon (2012) 139–163.

[10] R. Wagner, M. Robinson, Distribution, formation mechanisms, and significance of lunar pits, Icarus vol. 237 (2014) 52–60.

[11] T. Titus, J. Wynne, P. Boston, P. de Leon, C. Demirel-Floyd, H. Jones, F. Sauro, K. Uckert, A. Aghamohammadi, C. Alexander, Science and technology requirements to explore caves in our solar system, Bull. Amer. Astron. Soc. 53 (4) (2021a) 167.

[12] T. Titus, J. Wynne, M. Malaska, et al., A roadmap for planetary caves science and exploration, Nat. Astron. 5 (6) (2021b) 524–525.

[13] J. Blamont, A roadmap to cave dwelling on the moon and mars, Adv. Space Res. 54 (10) (2014) 2140–2149.

[14] ESA: Plans Mission to explore lunar caves, 2021, URL https://www.esa.int/Enabling_Support/Preparing_for_the_Future/Discovery_and_Preparation/ESA_plans_mission_to_explore_lunar_caves (accessed 23 August 2021).

[15] ESA: En Route to exploring lunar caves, 2020, URL https://www.esa.int/Enabling_Support/Preparing_for_the_Future/Discovery_and_Preparation/En_route_to_exploring_lunar_caves (accessed 22 August 2021).

[16] DAEDALUS: DEscent and exploration in deep autonomy of lava underground structures, 2021, URL https://www.informatik.uni-wuerzburg.de/space/mitarbeiter/nuechter/projects/daedalus/ (accessed 23 August 2021).

[17] DFKI: Skylight - Tethered micro rover for safe semi-autonomous exploration of lava tube, 2020, URL https://www.dfki.de/en/web/research/projects-and-publications/projects-overview/projekt/skylight/ (accessed 22 August 2021).

[18] W. Whittaker, Technologies Enabling Exploration of Skylights, Lava Tubes and Caves, Tech. Rep., NASA, 2012, URL https://www.nasa.gov/sites/default/files/atoms/files/niac_2011_phasei_whittaker_lavatubesandcaves_tagged.pdf (accessed 22 August 2021).

[19] M.Y. Metwly, M.S. Abdel-Majeed, A.S. Abdel-Khalik, R.A. Hamdy, M.S. Hamad, S. Ahmed, A review of integrated on-board EV battery chargers: Advanced topologies, recent developments and optimal selection of FSCW slot/Pole combination, IEEE Access 8 (2020) 85216–85242, Conference Name: IEEE Access.

[20] M. Shidujaman, L.T. Rodriguez, H. Samani, Design and navigation prospective for wireless power transmission robot, in: 2015 International Conference on Informatics, Electronics Vision (ICIEV), 2015, pp. 1–6.

[21] B. Zhou, S. Qian, Dynamics-based nonsingular interval model and luffing angular response field analysis of the dacs with narrowly bounded uncertainty, Nonlinear Dynam. 90 (2017) 2599—2626.

[22] B. Zhou, B. Zi, Y. Li, W. Zhu, Hybrid compound function/subinterval perturbation method for kinematic analysis of a dual-crane system with large bounded uncertainty, J. Comput. Nonlinear Dyn. 16 (1) (2021) 014501, (10 pages).

[23] NASA Announces lunar delivery challenge winners, 2021, URL https://www.nasa.gov/feature/nasa-announces-lunar-delivery-challenge-winners (accessed 24 August 2021).

[24] R. Bostelman, J. Albus, K. Murphy, T. Tsai, E. Amatucci, A stewart platform lunar rover, in: Proceedings of the Space '94 Conference, Albuquerque, NM, February 28-March 3, 1994.

[25] L. Solazzi, Z. Nenad, Design of a high capacity derrick crane considering the effects induced by load application and release, J. Appl. Eng. Sci. 15 (2017) 15–24.

[26] B. Boutin, A. Misra, V. Modi, Dynamics and control of variable-geometry truss structures, Acta Astronaut. 45 (12) (1999) 717–728.

[27] K. Miura, H. Furuya, K. Suzuki, Variable geometry truss and its application to deployable truss and space crane arm, Acta Astronaut. 12 (7-8) (1985) 599–607.

[28] P. Hughes, W. Sincarsin, K. Carroll, Trussarm - a variable-geometry-truss manipulator, J. Intell. Mater. Syst. Struct. 2 (2) (1991) 148–160.

[29] C. Gun-Shing, B.K. Wada, On an adaptive truss manipulator space crane concept, no. (a92-39251 16-39), in: Joint U.S./Japan Conference on Adaptive Structures, 1st, Maui, HI, Proceedings, Technomic Publishing Co., Inc., Lancaster, PA, 1990, pp. 726–742.

[30] J. Dorsey, T. Sutter, K. Wu, Structurally Adaptive Space Crane Concept for Assembling Space Systems on Orbit, Tech. Rep., 2003.

[31] Lightweight crane technology could find a home on the moon, 2021, URL https://www.nasa.gov/feature/langley/lightweight-crane-technology-could-find-a-home-on-the-moon (accessed 23 August 2021).

[32] Robotics automation and control lunar surface manipulation system (LAR-TOPS-73). Heavy lifting and precise positioning device, 2021, URL https://technology.nasa.gov/patent/LAR-TOPS-73 (accessed 22 August 2021).

[33] Esa: open space innovation platform - osip - campaign: system studies - lunar caves, 2021, URL https://ideas.esa.int/servlet/hype/IMT?documentTableId=45087640623196432&userAction=Browse&templateName=&documentId=d5e1d96887b7644587a60ba84f549af3 (accessed 24 August 2021).

[34] L. Kerber, I. Nesnas, L. Keszthelyi, J. Head, B. Denevi, P. Hayne, K. Mitchell, J. Ashley, J. Whitten, A. Stickle, Moon diver: A discovery mission concept for understanding the history of the mare basalts through the exploration of a lunar mare pit, New Views Moon 2 - Asia (2018).

[35] G. Podesta, Lunar nano drone for a mission of exploration of lava tubes on the moon: Propulsion system, Polit. Torino (2020) URL http://webthesis.biblio.polito.it/id/eprint/17038 (accessed 23 August 2021).

[36] P. Lee, J. Riedel, L. Jones-Wilson, E. Brandeau, C. O'Farrell, J. Gallon, Globe-trotter: An airbag hopper for mars surface and pit/cave exploration, Space Sci. 58 (2019) 592–598.

[37] J. Thangavelautham, M. Robinson, A. Taits, T. McKinney, S. Amidan, A. Polak, Flying, hopping pit-bots for cave and lava tube exploration on the moon and mars, 2017.

[38] M. Merz, A.A. Transeth, G. Johansen, M. Bjerkeng, Snake robots for space applications, 0000, 6.

[39] A.K. Theinat, A. Modiriasari, A. Bobet, H.J. Melosh, S.J. Dyke, J. Ramirez, A. Maghareh, D. Gomez, Lunar lava tubes: Morphology to structural stability, Icarus 338 (2020) 113442.

[40] N. Sun, Y. Wu, Y. Fang, H. Chen, Nonlinear antiswing control for crane systems with double-pendulum swing effects and uncertain parameters: Design and experiments, IEEE Trans. Autom. Sci. Eng. 15 (3) (2018) 1413–1422.

[41] L. Yliniemi, A.K. Agogino, K. Tumer, Multirobot coordination for space exploration, AI Mag. 35 (4) (2014) 61–74.

[42] A. Kisdi, A. Tatnall, Future robotic exploration using honeybee search strategy: Example search for caves on mars, Acta Astronaut. 68 (11) (2011) 1790–1799.

[43] P. Nannipieri, L. Fanucci, F. Siegle, A representative SpaceFibre network evaluation: Features, performances and future trends, Acta Astronaut. 176 (2020) 313–323.

[44] A. Hrovat, G. Kandus, T. Javornik, A survey of radio propagation modeling for tunnels, IEEE Commun. Surv. Tutor. 16 (2) (2014) 658–669.

[45] S. Betrencourt, M. Lienard, P. Degauque, D. Degardin, Mobile communication in road tunnels: influence of the traffic conditions on the channel characteristics, in: 2000 10th Mediterranean Electrotechnical Conference. Information Technology and Electrotechnology for the Mediterranean Countries. Proceedings. MeleCon 2000 (Cat. No.00CH37099), Vol. 1, 2000, pp. 432–435, vol.1.

[46] J. Feng, Y. Su, C. Ding, S. Xing, S. Dai, Y. Zou, Dielectric properties estimation of the lunar regolith at CE-3 landing site using lunar penetrating radar data, Icarus 284 (2017) 424–430.

[47] L. Turchi, S.J. Payler, F. Sauro, R. Pozzobon, M. Massironi, L. Bessone, The electronic FieldBook: A system for supporting distributed field science operations during astronaut training and human planetary exploration, Planet. Space Sci. 197 (2021) 105164.

[48] J. Haruyama, S. Sawai, T. Mizuno, T. Yoshimitsu, S. Fukuda, I. Nakatani, Exploration of lunar holes, possible skylights of underlying lava tubes, by smart lander for investigating moon (SLIM), Trans. Jpn. Soc. Aeronaut. Space Sci. Aerosp. Technol. Jpn. 10 (ists28) (2012) Pk_7–Pk_10.

[49] T. Hirata, K. Tsujita, Simulation study on supporting condition of a robotic gravity compensation system for the prototype test of spacecraft, in: 18th International Conference on Advanced Robotics (ICAR), 2017, pp. 322–327.

[50] K. Tsujita, H. Shigematsu, N. Kishimoto, Development of gravity compensation system for the prototype test of deployable space structure by using multi robot, 2016.

[51] Z. Zhao, K. Fu, M. Li, J. Li, Y. Xiao, Gravity compensation system of mesh antennas for in-orbit prediction of deployment dynamics, Acta Astronaut. 167 (2020) 1–13.

[52] Z. Liu, H. Gao, Z. Deng, Design and implementation of a large-scale gravity compensation system for lunar rover, Appl. Mech. Mater. 385–386 (2013) 759–767.